Molecular Crystals and Liquid Crystals
Publication details, including instructions for authors and subscription information:
http://www.tandfonline.com/loi/gmcl18

Liquid Crystalline Cores for Optical Fibers

H. Lin [a] , P. Palffy-muhoray [a] & Michael A. Lee [a]
[a] Liquid Crystal Institute and Department of Physics, Kent State University, Kent, Ohio, 44242, USA
Version of record first published: 04 Oct 2006.

To cite this article: H. Lin , P. Palffy-muhoray & Michael A. Lee (1991): Liquid Crystalline Cores for Optical Fibers, Molecular Crystals and Liquid Crystals, 204:1, 189-200

To link to this article: http://dx.doi.org/10.1080/00268949108046605

Mol. Cryst. Liq. Cryst., 1991, Vol. 204, pp. 189–200
Reprints available directly from the publisher
Photocopying permitted by license only

Printed in the United States of America

Liquid Crystalline Cores for Optical Fibers

H. LIN, P. PALFFY-MUHORAY and MICHAEL A. LEE

Liquid Crystal Institute and Department of Physics, Kent State University, Kent, Ohio, USA 44242

(Received September 17, 1990)

We consider the problem of wave guiding by optical fibers with nematic liquid crystal cores. The dielectric properties of the core which govern wave guiding in the fiber are determined by the nematic director field. We focus on the problem of determining the configuration of the liquid crystal in a cylindrical cavity with homeotropic boundary conditions. Using the Frank free energy, we find a transition from a radial to an axial structure. The order parameter field in the radial structure is also examined. If the core radius is greater than an optical wavelength, then, away from the nematic-isotropic transition, the free energy of the axial structure is smaller than that of the radial one. The dielectric tensor corresponding to the axial configuration is both inhomogeneous and anisotropic. We derive uncoupled wave equations for the TE and TM modes, and we propose an effective numerical method to obtain solutions.

I. INTRODUCTION

The basic configuration of an optical fiber waveguide is a cylindrical core with index of refraction n, coated with a cladding material of refractive index n_c ($n > n_c$). Much attention[1-4] has been focused recently on optical fibers with optically linear and nonlinear crystalline cores. In this work, we consider optical fibers with liquid crystalline cores, where the liquid crystal is both an inhomogeneous and anisotropic medium. The optical properties of the cylindrical waveguide depend on the dielectric permittivity of the core.

To determine the configuration of the liquid crystal in the core, we compare the Frank free energy of a radial and an axial structure in Sec. II. In Sec. III we study the order parameter profile of the radial structure using the Landau-de Gennes free energy. Since for core radii and temperatures of practical interest it is the axial structure which is stable, we consider the problem of wave propagation for this structure in Sec. IV.

II. DIRECTOR FIELDS AND CONFIGURATIONAL TRANSITIONS

We consider a nematic liquid crystal confined in a cylinder with radius R, and take the symmetry axis of cylinder as the z axis. The director field configurations in a cylinder are determined by elastic torques and surface interactions. In the case of

rigid homeotropic alignment of the director on the surface of the cylinder, we consider two director field configurations: one with cylindrical symmetry with no central singularity (axial structure); and another with a radial configuration and an isotropic core (radial structure). Both configurations are shown in Figure 1.

We start with the Frank free energy density[6] which assumes that the orientational order parameter S is constant,

$$f = \frac{1}{2}[K_1(\nabla \cdot \hat{n})^2 + K_2(\hat{n} \cdot \nabla \times \hat{n})^2 + K_3(\hat{n} \times \nabla \times \hat{n})^2] \tag{1}$$

where K_1, K_2 and K_3 are elastic constants and $\hat{n}(\vec{r})$ is the spatially varying director field. In cylindrical coordinates, the director field for the axial structure is given by

$$\hat{n} = \hat{n}(\sin\theta, 0, \cos\theta) \tag{2}$$

where θ is the angle between the director and the symmetry axis of cylinder. We assume that θ only depends on the radial coordinate r, and that $\theta(R) = \pi/2$, $0 \leqslant r \leqslant R$.

Substituting this expression into Equation 1, we obtain the free energy density expression for the axial structure

$$f = \frac{1}{2}[(K_3 - K_1)\sin^2\theta + K_1]\left(\frac{\partial\theta}{\partial r}\right)^2 + \frac{K_1}{2}\frac{\sin 2\theta}{r}\frac{\partial\theta}{\partial r} + \frac{K_1}{2}\frac{\sin^2\theta}{r^2} \tag{3}$$

Minimizing this free energy gives rise to the partial differential equation

$$2r^2 g(\theta)\frac{\partial^2\theta}{\partial r^2} + r^2(\nu - 1)\sin 2\theta\left(\frac{\partial\theta}{\partial r}\right)^2 + 2rg(\theta)\frac{\partial\theta}{\partial r} - \sin 2\theta = 0 \tag{4}$$

where $g(\theta) = 1 + (\nu - 1)\sin^2\theta$, and $\nu = K_3/K_1$.

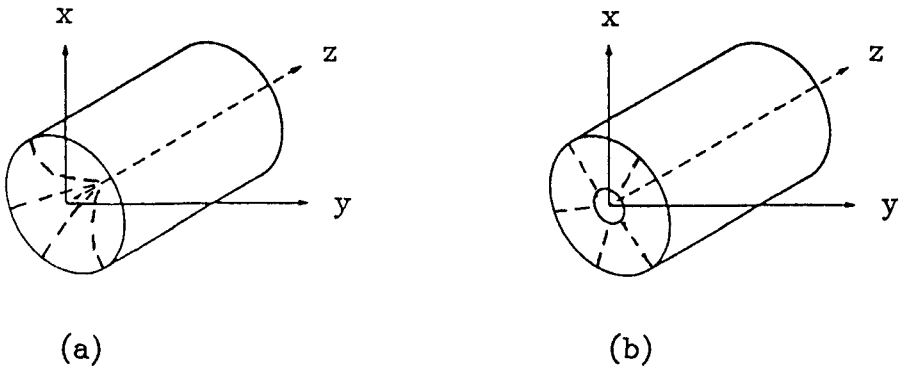

(a) (b)

FIGURE 1 Director configurations (a)axial structure, (b)radial structure.

Equation 4 is a nonlinear equation, which we solve numerically. Although analytical methods are viable here,[7] we anticipate the presence of fields which may influence $\hat{n}(\vec{r})$. These can be included with relatively minor modifications of our numerical method, but could not be easily accommodated in the analytical solution. We used the shooting method; results for θ vs. r for different values of ν are shown in Figure 2. From the expression for $\hat{n}$ in Equation 2 the dielectric tensor $\bar{\bar{\varepsilon}}$ has the form

$$\bar{\bar{\varepsilon}} = \begin{bmatrix} \varepsilon_{rr} & 0 & \varepsilon_{rz} \\ 0 & \varepsilon_{\phi\phi} & 0 \\ \varepsilon_{zr} & 0 & \varepsilon_{zz} \end{bmatrix} \tag{5}$$

where $\varepsilon_{rr} = \varepsilon_\perp + \Delta\varepsilon \sin^2\theta$, $\varepsilon_{rz} = \varepsilon_{zr} = \Delta\varepsilon \sin\theta \cos\theta$, $\varepsilon_{\phi\phi} = \varepsilon_\perp$, $\varepsilon_{zz} = \varepsilon_\perp + \Delta\varepsilon \cos^2\theta$, and $\Delta\varepsilon = \varepsilon_\parallel - \varepsilon_\perp$. $\varepsilon_\parallel$ and $\varepsilon_\perp$ refer to the dielectric constant for polarization parallel and perpendicular to the symmetry axis, respectively. So the elements of the dielectric tensor matrix are a function of position, and determined by the director field configuration.

When $K_1 = K_3$, there exists the closed form solution $\theta = 2\tan^{-1}(r/R)$, as shown by Cladis and Kleman,[7] and the free energy per unit length

$$F_a = 3\pi K \tag{6}$$

is a constant.

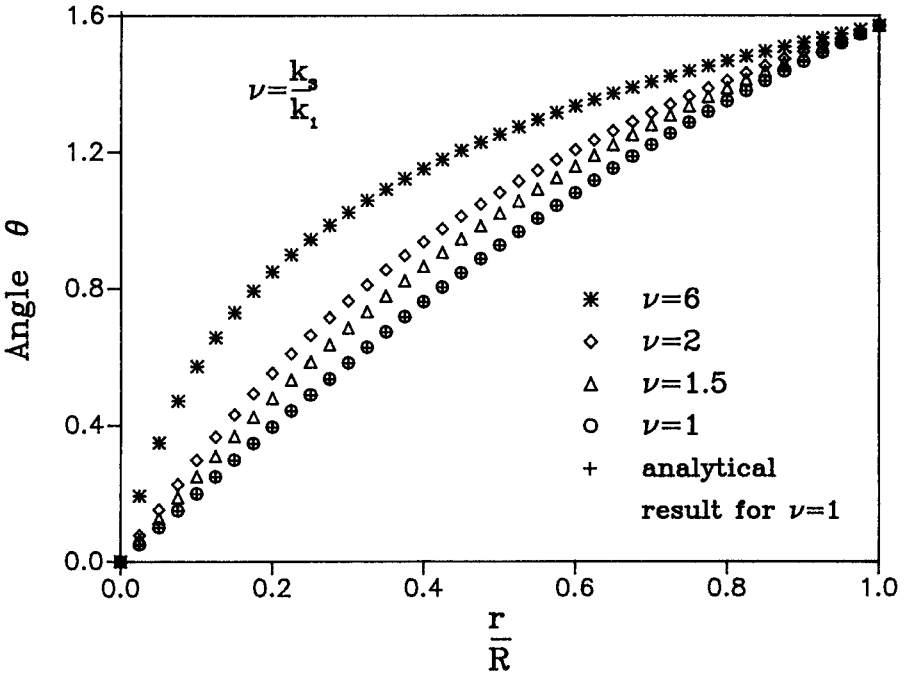

FIGURE 2 Director fields in cylinder for an axial structure.

We next consider the radial structure, where we assume that an isotropic region exists near the axis of the cylinder for $r < r_0$ due to the large elastic curvature. The director field $\hat{n}(\vec{r})$ in this structure is

$$\hat{n} = \hat{n}(1, 0, 0). \tag{7}$$

The free energy per unit length, taking into account the interfacial energy as well as the energy difference between the nematic and isotropic phases, is

$$F_r = \pi K_1 \ln \frac{R}{r_0} + 2\pi\sigma r_0 + \pi\Delta r_0^2 \tag{8}$$

The first term is the splay term from the Frank free energy expression, σ is the nematic-isotropic (*N-I*) interfacial energy, Δ is the free energy difference between nematic and isotropic phases, and r_0 is the radius of the isotropic core.

Minimizing F_r with respect to r_0 and solving the resulting quadratic equation, we obtain

$$r_0 = \frac{\sigma}{2\Delta}\left[-1 + \sqrt{1 + \frac{2\Delta K_1}{\sigma^2}}\right] \tag{9}$$

where $\Delta = L(T - T_{NI})$, L is the latent heat per volume and T_{NI} is the nematic-isotropic transition temperature.

Substituting Equation 9 into Equation 8, we obtain

$$F_r = \pi K_1 \ln \frac{R}{r_0} + \pi\sigma r_0 + \frac{1}{2}\pi K_1 \tag{10}$$

From the crossover of the free energy for the two configurations, given by Equations 6 and 10, we arrive at the condition

$$R_c = r_0 \exp\left(\frac{5}{2} - \frac{\sigma}{K} r_0\right) \tag{11}$$

for the transition from a radial to an axial structure.

When the temperature approaches the *N-I* transition temperature, i.e., $\Delta \to 0$, then from Equation 9,

$$r_0 = \frac{K}{2\sigma} \tag{12}$$

and

$$R_c = \frac{K}{2\sigma} e^2 \tag{13}$$

At the nematic isotropic transition, K and σ both have non-zero values; thus r_0 remains finite. As the temperature decreases below the transition, K and σ remain essentially constant while Δ increases, and from Equation 9 one sees that r_0 decreases with temperature. The value of r_0 may be estimated from the material constants for 8CB. Here $K = 10^{-12} N$, $\sigma = 9 \times 10^{-6}$ J/m^2, and from Equations 12 and 13, $r_0 = 0.056$ μm and $R_c = 0.41$ μm.

When $R \leqslant R_c$, the director field configuration favors the radial structure with the isotropic core; and when $R \geqslant R_c$, the axial structure is energetically favourable. We expect therefore that even at the *N-I* transition, the axial structure is favoured for large R ($R \gtrsim 0.5$ μm), and that this structure remains favorable for even smaller values of R as the temperature is lowered.

One interesting exception is the case of materials (such as 8CB) which have a smectic phase below the nematic phase. In these materials K_3 diverges as the nematic-smectic transition is approached, and the free energy per unit length of the axial structure diverges. In these materials, the radial structure is expected to be favorable, even for very large values of R, very near (and in) the smectic phase.

III. ORDER PARAMETER TRANSITIONS

Because of the assumption of constant order parameter S, the free energy expression of Equation 8 is only approximate. It is interesting to consider the effects of spatial variations of S. The Landau-de Gennes free energy density of the radial structure is

$$f = \frac{1}{2} AS^2 - \frac{1}{3} BS^3 + \frac{1}{4} CS^4 + \frac{LS^2}{2r^2} + \frac{L}{2}\left(\frac{\partial S}{\partial r}\right)^2 + f_s \tag{14}$$

in the single elastic constant approximation. Here L is an elastic constant, and f_s is the surface contribution,[8] given by

$$f_s = -GS(r)\delta(r - R), \tag{15}$$

and $A = a(T - T_0) = a\Delta T$, T is the temperature. a, T_0, B, C and L are material parameters which can be determined from thermodynamic and fluctuation measurements.

Minimizing the free energy results in

$$\frac{\partial^2 S}{\partial r^2} + \frac{1}{r}\frac{\partial S}{\partial r} - \frac{1}{L}(AS - BS^2 + CS^3) - \frac{S}{r^2} = 0 \tag{16}$$

with the boundary condition $\partial S/\partial r = G/L$ at $r = R$. We use a relaxation method to solve Equation 16 for the set of parameters[5] $a = 0.1319 \times 10^5$ J/m^{3}K, $B = 1.836 \times 10^5$ J/m^3, $C = 4.050 \times 10^9$ J/m^3, $L = 2.7 \times 10^{-11}$ J/m, $T_0 = 307$ K. The spatial dependence of the order parameter $S(r)$ is given in Figures 3, 4 and 5, where $g = G/L$.

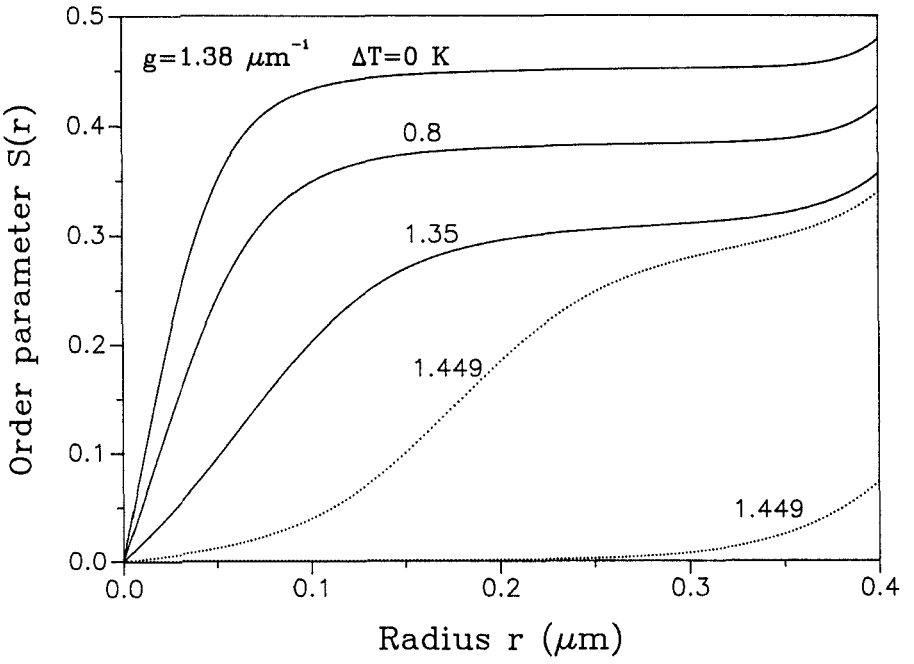

FIGURE 3 Spatial dependence of the order parameter.

From these Figures, we see that the order parameter is zero if $r \simeq 0$, due to the large elastic deformation near the cylinder axis. The spatial dependence of $S(r)$ and the order parameter transitions depend on the surface anchoring strength G, the radius of the cylinder R and the temperature difference ΔT. As the temperature is lowered, we see two transitions. One is a surface transition, where the order parameter at the cylinder surface increases discontinuously, the second is a bulk transition corresponding to the discontinuous increase of the order parameter in the region bounded by the center and surface of the cylinder. Both transitions are first order; that is, two solutions coexist for some range of temperatures. In Figure 6 we show the average order parameter, averaged over the volume of the cell, as the temperature was increased and decreased. The hysteresis confirms that the transitions are indeed first order; the transition temperature can be determined exactly by comparing the free energies of the solutions.

IV. WAVE PROPAGATION IN OPTICAL FIBERS

The wave propagation in dielectric waveguides is described by solutions of Maxwell's equations with appropriate boundary conditions at the core-cladding interface. The dielectric properties of the core material enter via the dielectric tensor. Analytical solutions to the cylindrical waveguide problems can be obtained for an isotropic and homogeneous core in an infinitely large cladding.[10] In our case, the

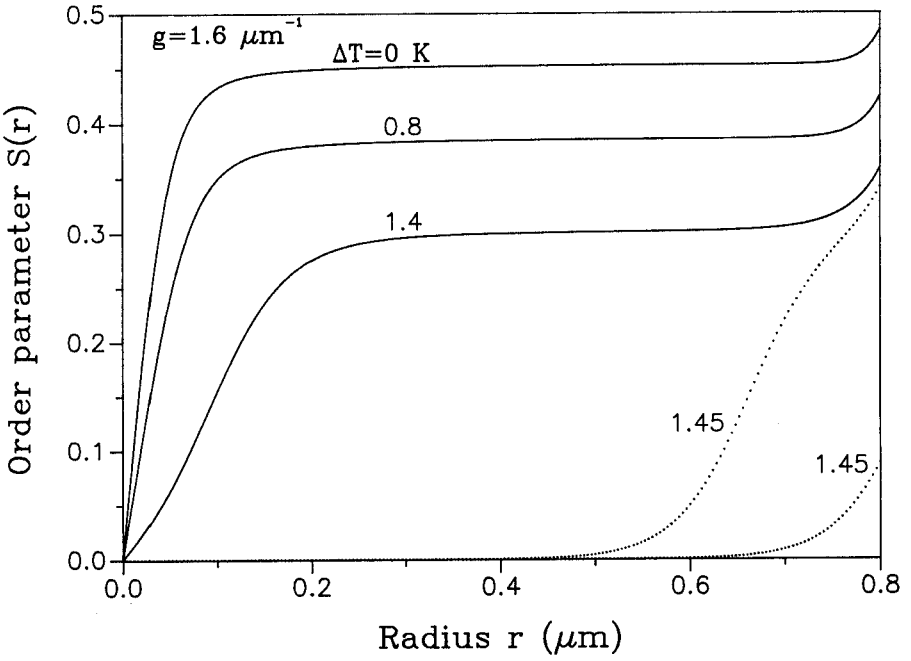

FIGURE 4 Spatial dependence of the order parameter.

liquid crystal core is both anisotropic and inhomogeneous, and consequently the wave equation has to be solved numerically.

The model cylindrical dielectric waveguide consists of a cylindrically symmetric core region with radius R, containing the nematic liquid crystal, and surrounded by an isotropic cladding with dielectric constant ε_c extending to infinity. The magnetic permeabilities of both are assumed to be the same as that of free space, that is, $\mu = \mu_0$. The dielectric permittivity of the liquid crystal core is a spatially varying tensor. In cylindrical coordinates, if the z axis is taken along the direction of symmetry axis of the waveguide, the dielectric tensor $\bar{\bar{\varepsilon}}$ is given by Equation 5. The angle $\theta(r)$ is obtained by solving Equation 4.

To derive the wave equations, we start with Maxwell's equations

$$\nabla \times \vec{E} = -\frac{\partial \vec{B}}{\partial t} \tag{17}$$

$$\nabla \times \vec{H} = \frac{\partial \vec{D}}{\partial t} \tag{18}$$

$$\nabla \cdot \vec{D} = 0 \tag{19}$$

$$\nabla \cdot \vec{H} = 0 \tag{20}$$

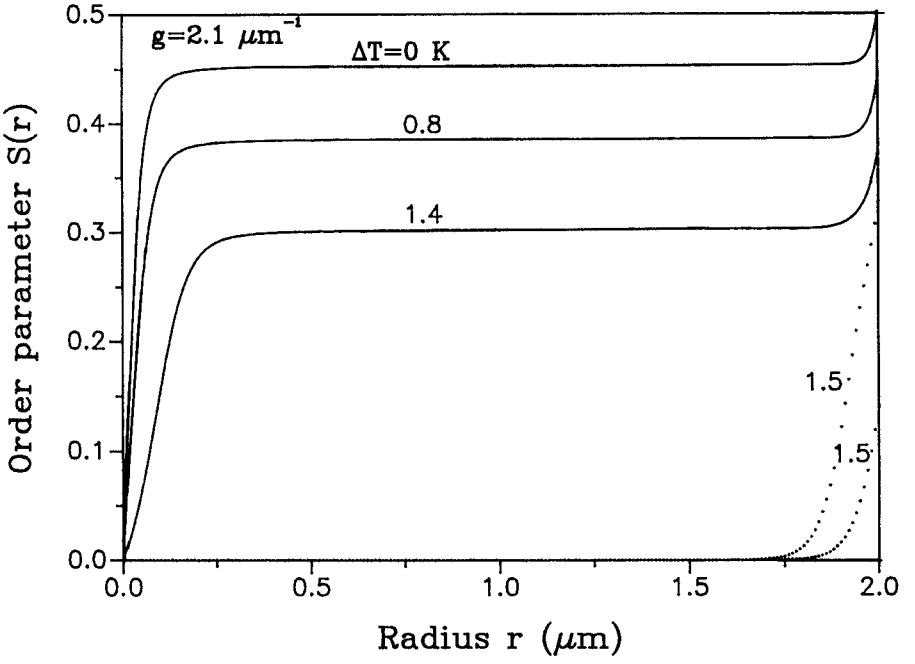

FIGURE 5 Spatial dependence of the order parameter.

where the displacement vector $\vec{D}$ and the electric field vector $\vec{E}$ are related by

$$\vec{D} = \varepsilon_0 \bar{\bar{\varepsilon}} \vec{E} \tag{21}$$

where ε_0 is the permittivity of free space. The magnetic flux density $\vec{B}$ and the magnetic field $\vec{H}$ are related by

$$\vec{B} = \mu_0 \vec{H} \tag{22}$$

where μ_0 is the permeability.

In order to obtain uncoupled equations, we consider the case where the fields have no azimuthal variation. Then, in cylindrical coordinates, the fields in Equations 17–22 are assumed to have a sinusoidal time dependence and to propagate along z axis, and are given by

$$\vec{F}(\vec{r}, z, \phi) = \vec{F}(r) e^{i(\omega t - \beta z)} \tag{23}$$

where $\vec{F}$ denotes $\vec{E}$ or $\vec{H}$, ω is the optical frequency and β is propagation factor.

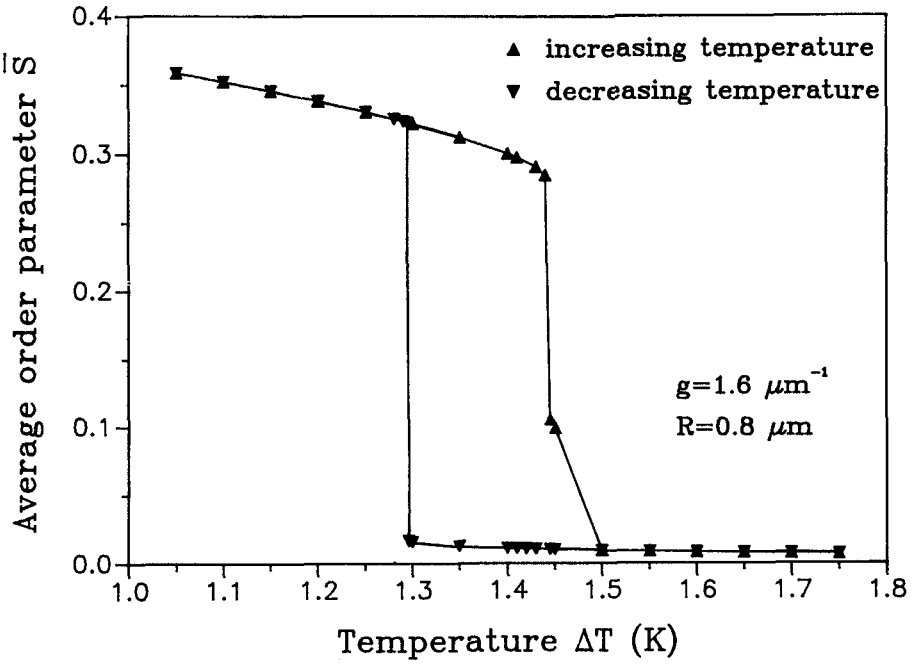

FIGURE 6 Average order parameter as function of temperature.

Using Equations 21, 22 and the set of Maxwell's Equations, we derived the uncoupled wave equations for TE modes

$$\frac{\partial^2 E_\Phi}{\partial r^2} + \frac{1}{r}\frac{\partial E_\Phi}{\partial r} + \left(\omega^2\mu\varepsilon - \beta^2 - \frac{1}{r^2}\right) E_\Phi = 0 \tag{24}$$

$$H_r = -\frac{\beta}{\omega\mu} E_\Phi \tag{25}$$

$$H_z = \frac{i}{\omega\mu}\left(\frac{\partial E_\Phi}{\partial r} + \frac{E_\Phi}{r}\right). \tag{26}$$

For these modes, the anisotropy of the core does not enter into the equations, since E_Φ is always perpendicular to $\hat{n}$, and hence $\varepsilon = \varepsilon_\perp$ for the core. In the cladding $\varepsilon = \varepsilon_c$. For the TE modes, the boundary conditions at the liquid crystal-cladding interface are given by

$$E_\Phi = E'_\Phi \tag{27}$$

$$\frac{\partial E_\Phi}{\partial r} = \frac{\partial E'_\Phi}{\partial r} \tag{28}$$

on the boundary $r = R$, and E_Φ denotes the field inside the core, and E'_Φ in the cladding.

The equations for the TM modes inside the core are

$$\frac{\partial^2 H_\phi}{\partial r^2} + \left(\frac{1}{r} + \frac{1}{\varepsilon_{rr}}\frac{\partial \varepsilon_{rr}}{\partial r} - 2i\beta\frac{\varepsilon_{rz}}{\varepsilon_{rr}}\right)\frac{\partial H_\phi}{\partial r}$$

$$+ \left[\omega^2\mu\frac{\varepsilon_\parallel\varepsilon_\perp}{\varepsilon_{rr}} - \beta^2\frac{\varepsilon_{zz}}{\varepsilon_{rr}} - \frac{1}{r^2} - \frac{i\beta}{\varepsilon_{rr}}\left(\frac{\partial \varepsilon_{rz}}{\partial r} + \frac{\varepsilon_{rz}}{r}\right) + \frac{1}{r\varepsilon_{rr}}\frac{\partial \varepsilon_{rr}}{\partial r}\right] H_\phi = 0 \quad (29)$$

$$E_r = \frac{1}{i\omega\varepsilon_\parallel\varepsilon_\perp}\left[i\beta\varepsilon_{zz}H_\phi - \varepsilon_{rz}\left(\frac{\partial H_\phi}{\partial r} + \frac{H_\phi}{r}\right)\right] \quad (30)$$

$$E_z = \frac{i}{\omega\varepsilon_\parallel\varepsilon_\perp}\left[i\beta\varepsilon_{rz}H_\phi - \varepsilon_{rr}\left(\frac{\partial H_\phi}{\partial r} + \frac{H_\phi}{r}\right)\right] \quad (31)$$

and outside

$$\frac{\partial^2 H_\phi}{\partial r^2} + \frac{1}{r}\frac{\partial H_\phi}{\partial r} + \left(\omega^2\mu\varepsilon_c - \beta^2 - \frac{1}{r^2}\right) H_\phi = 0 \quad (32)$$

$$E_r = -\frac{\beta}{\omega\varepsilon_c} H_\phi \quad (33)$$

$$E_z = -\frac{i}{\omega\varepsilon_c}\left(\frac{\partial H_\phi}{\partial r} + \frac{H_\phi}{r}\right) \quad (34)$$

The complex coefficients in Equation 29 arise from the inhomogeneous and anisotropic core, these require that H_ϕ be complex function of position. This means that the phases of both electric and magnetic fields vary with r.

For the TM modes, the boundary conditions at the liquid crystal-cladding interface are given by

$$H_\phi = H'_\phi \quad (35)$$

$$\left(\frac{\partial H_\phi}{\partial r} + \frac{H_\phi}{r}\right) = \left(\frac{\partial H'_\phi}{\partial r} + \frac{H'_\phi}{r}\right) \quad (36)$$

on the boundary $r = R$, and H_ϕ denotes the field inside the core, and H'_ϕ in the cladding.

From the Equations 24–26, we can see that an analytical solution of TE mode can be obtained for the infinite cladding. In fact, the equations for TE_{0m} modes are of the same form as those in an isotropic and homogeneous case.[10] So for $r < R$, the azimuthal component E_ϕ in the core becomes

$$E_\phi = AJ_1(\alpha r) \quad (37)$$

which is the first order Bessel function with an amplitude constant A, and for $r > R$, E_ϕ outside is

$$E_\phi = K_1^{(1)}(\gamma r) \tag{38}$$

which is the first kind modified Hankel function with a chosen unity amplitude constant, and where α and γ are defined by $\alpha^2 = \omega^2\mu\varepsilon_\perp - \beta^2$, $\gamma^2 = \beta^2 - \omega^2\mu\varepsilon_c$, respectively, β is the propagation constant. The magnetic components H_r and H_z are expressed by Equations 25 and 26.

Matching the tangential components E_ϕ and E_z at the core-cladding interface leads to the eigenvalue equation

$$\frac{J_1(\alpha R)}{\alpha R J_0(\alpha R)} + \frac{K_1^{(1)}(\gamma R)}{\gamma R K_0^{(1)}(\gamma R)} = 0 \tag{39}$$

which determines the propagation constants of the guided modes TE_{0m}. The field distributions of the TE_{0m} modes can be obtained when β is obtained from Equation 39.

The equations for the TM modes must be solved numerically. We have developed a modified shooting method for this purpose, where the eigenvalue β is varied instead of the slope at the boundary. Using this method, we have obtained nu-

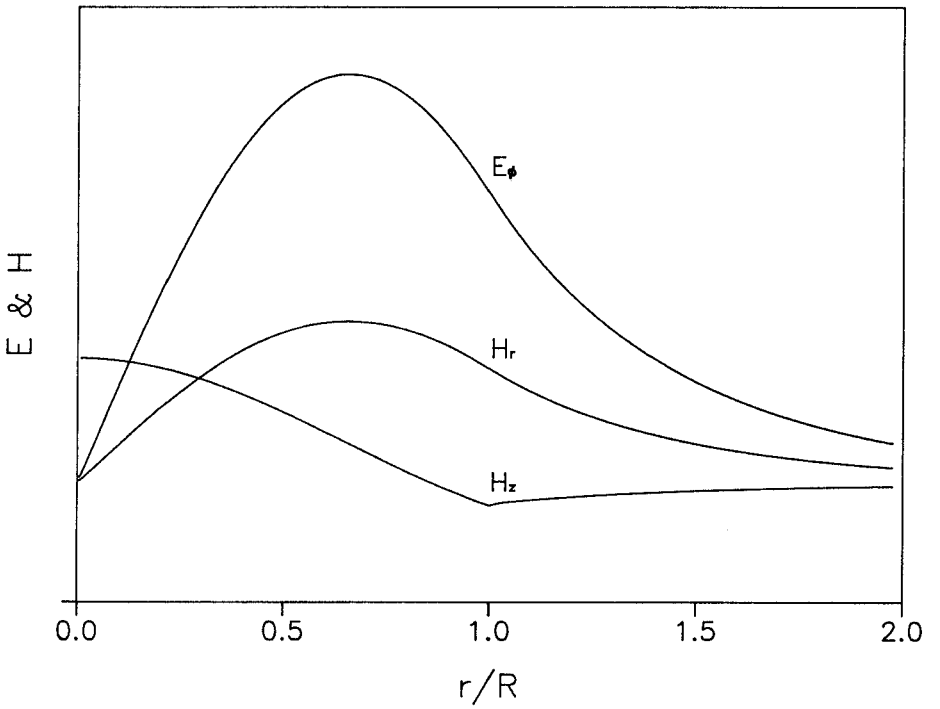

FIGURE 7 Field distributions of TE_{01} mode.

merical solutions for the TE modes. Figure 7 shows the field distributions of TE_{01} mode; it is in excellent agreement with the analytical results of Equations 37 and 38. Preliminary results suggest that our modified shooting method can be used to obtain solutions for the TM modes. Results of these calculations, as well as details of the shooting procedure will be presented elsewhere.

V. CONCLUSION

We have calculated the director configuration in nematic liquid crystal samples confined in a cylindrical geometry, and determined the dielectric tensor as a function of position. We have found a transition from a radial to an axially symmetric structure for certain values of the parameters. Our results indicate that for large capillaries at temperatures well below the NI transition, the director 'escapes into the third dimension'; the director field gradients are small and the assumption of constant order parameter S is justified. In addition, we have found that in the radial configuration, the orientational order parameter is spatially inhomogeneous, and for certain values of parameters exhibits a discontinuous surface and bulk phase transitions. Similar phenomena have been reported in a spherical geometry by Allender and Zumer.[9]

We have considered wave propagation in optical fibers with anisotropic and inhomogeneous cores. For TE and TM modes in the axial structure, the wave equations are decoupled, and we have developed a numerical technique to solve these equations. Work to obtain solutions of the coupled equations is still under way.

Acknowledgment

This work was supported by DARPA through US Army CECOM Center for Night Vision and Electro-Optics. We acknowledge useful discussions with J. Kelly of the Liquid Crystal Institute at Kent State University.

References

1. P. V. Vidakovic, M. Coquilay and F. Salin, *J. Opt. Soc. Am. B*, Vol. **4**, No. 6, 998 (1987).
2. M. D. Feit and J. A. Fleck, Jr., *Opt. Lett.*, **14**, 662 (1989).
3. J. L. Stevenson and R. B. Dyott, *Electron. Letts.*, **10**, 449 (1974).
4. B. K. Nayar, *Springer Proceedings in Physics*, **7**, 142 (1985).
5. P. G. de Gennes, *The Physics of Liquid Crystals*, (Clarendon, 1974).
6. F. C. Frank, *Faraday Soc. Disc.*, **25**, 19 (1958).
7. P. E. Cladis and M. Kleman, *J. de Physique*, **33**, 591 (1972).
8. P. Sheng, *Phys. Rev. A26*, 1610 (1982).
9. D. W. Allender and S. Zumer, SPIE Proceedings, Vol. 1080, 18 (1989).
10. D. Marcuse: Theory of Dielectric Optical Waveguides (Academic, New York 1974).